

The radial dependence of dark matter distribution in M33

E. López Fune,^{1 2*} P. Salucci,^{1 3†} E. Corbelli,^{4‡}

¹*Scuola Internazionale Superiore di Studi Avanzati (SISSA). Via Bonomea, # 265, 34136 Trieste, Italy.*

²*Abdus Salam International Centre for Theoretical Physics. Strada Costiera #11, 34151 Trieste, Italy.*

³*INFN, Sezione di Trieste. Via Valerio 2, 34127, Trieste, Italy.*

⁴*INAF-Osservatorio Astrofisico di Arcetri. Largo E. Fermi, 5, 50125 Firenze, Italy.*

Accepted XXX. Received YYY; in original form ZZZ

ABSTRACT

The stellar and gaseous mass distributions, as well as the extended rotation curve in the nearby galaxy M33 are used to derive the radial distribution of dark matter density in the halo and to test cosmological models of galaxy formation and evolution. Two methods are examined to constrain dark mass density profiles. The first deals directly with fitting the rotation curve data in the range of galacto-centric distances $0.24 \text{ kpc} \leq r \leq 22.72 \text{ kpc}$. As found in a previous paper by Corbelli *et al.* (2014), and using the results of recent collisionless Λ –CDM numerical simulations, we confirm that the Navarro-Frenkel-White (hereafter NFW) dark matter profile provides a marginally better fit to the rotation curve data than the cored Burkert profile, also called the Universal Rotation Curve (hereafter URC) profile. The second method relies on the local equation of centrifugal equilibrium and on the rotation curve slope. In the aforementioned range of distances, we fit the observed velocity profile using a function which has a rational dependence on the radius. Following Salucci *et al.* (2010), we then derive an expression for the slope of the rotation curve and for the radial dependence of the local dark matter distribution. In the radial range $9.53 \text{ kpc} \leq r \leq 22.72 \text{ kpc}$, where the uncertainties induced by the luminous matter (stars and gas) start to become negligible, we tested the NFW and the URC dark matter profiles. With this second method we confirm that both profiles are compatible with the data even though in this case the cored Burkert mass density profile provides a more reasonable value for the barionic-to dark matter ratio.

Key words: Galaxies: individual (M33) – Galaxies: ISM – Galaxies: kinematics and dynamics – dark matter

1 INTRODUCTION

In the innermost parts of galaxy disks, ranging between 1 and 3 disk exponential length-scales, according to the galaxy luminosity (Salucci *et al.* 1999), the luminous matter dominates the kinematics: light traces the mass (Athanassoula *et al.* 1987; Persic *et al.* 1988; Palunas *et al.* 2000). Instead in the outer skirts, far from galaxy centers, rotational velocities are found to be constant or even rising with radius despite the faint stellar or gaseous surface brightness. This contradicts the well known keplerian-like expectations of the standard Newtonian Gravity if light traces the mass. It is well known that, in order to explain this anomaly, a dark matter (hereafter DM) halo is routinely added in the computation of the gravitational potential (Bosma *et al.* 2000; Bosma *et al.* 1979; Rubin *et al.* 1980). The luminous and dark matter contribution to the rotation curve (hereafter RC) can explain the observed velocities as traced by star light or gas emission, even at large galactocentric distances where rotational velocities are flat or increase with radius.

On the other hand, it is well known that collisionless and stable Weakly Interacting Massive Particles (WIMPs) in

* E-mail: elopez@sissa.it

† E-mail: salucci@sissa.it

‡ E-mail: edvige@arcetri.astro.it

a Λ -CDM (Cold Dark Matter) cosmology, provide a major scenario to frame the DM in galaxies and in the Universe. Cosmological simulations show that the DM density distribution ρ_{DM} is nearly universal, i.e. dependent only on the mass of the halo. This density profile have a characteristic steep slope in the inner galactic regions which can be approximated by the power-law $\rho(r)/\rho_c \simeq (r/r_c)^{-\gamma}$, with ρ_c a characteristic constant density and r_c the constant scaling radius.

This cuspy density profile does not show up in a number of dwarfs, spirals and LSB galaxies (Burkert A. 1995; Salucci P. et. al. 2000; de Blok W. J. G. et. al. 2002; Gentile G. et. al. 2004, 2005) in favor of a much shallower cored profile. However, because the inner regions of galaxies are dominated by the luminous matter and most of the DM halo extends well outside the (rotating) stellar disk, the DM density profile is accurately derived only in a very small fraction of objects and most of the evidence for a cored distribution comes from stacked RCs. In this situation, the evidence of many stacked solid body RCs leading to a solid body profile $V \propto r$ at $r \rightarrow 0$ maybe not sufficient to determine the nature of dark matter. One needs, in fact, very accurate and complete mass models also of individual kinematics. This would require to have, for the same galaxy, an inner RC, usually traced by mm or optical lines, and a very extended RC traced by 21cm emission. For the debated issue about a core or cusp dark matter profile i we must report the recent results of numerical simulations: baryonic feedback occurring at a later times than galaxy formation period can transform the original NFW profiles into cored ones (Chan T. K. et. al. 2015). Hence, the evidence of cores for DM halo density distributions in dwarf galaxies is not sufficient to disprove the Λ -CDM scenario. The cusp-core issue in galaxy DM density profiles, also related to the investigation of the nature of DM itself, require the investigateion of galaxies of different Hubble type, luminosity and morphology.

In this paper we study in detail the DM distribution in the spiral galaxy M33. This object gives us the possibility of accurately deriving the DM halo distribution out to large distances and therefore to uniquely test the Λ -CDM cosmological scenario. This spiral hosts no bulge nor a prominent bar (Corbelli E. et. al. 2007): the absence of these concentrated stellar distributions much alleviates the usual uncertainty in deconvolving the disk contribution from that of a bulge, and of modelling correctly non circular motion. M33 is a low-luminosity spiral galaxy rich in gas and very much dark matter dominated: both properties make easy to track its dark component. Its rotation curve is very extended due to the presence of a large gaseous disc and has an excellent spatial resolution due to its proximity and to the presence of CO-lines that trace the inner kinematics (Corbelli E. 2003; Corbelli E. et. al. 2014). It is important to stress the crucial result obtained for this object by Corbelli E. et. al. (2014). They have inferred the stellar mass surface density as function of the galactocentric radius by means of the measured pixel-SED (Spectral Energy Distribution) and proper population synthesis models. This provides a good estimate of the stellar mass distribution in the M33, in particular of its radial profile, which previously has been assumed proportional to the luminosity one. This reduces considerably the uncertainties on the contribution of luminous matter to the galaxy circular velocity (Corbelli E. et. al. 2014). The gaseous disk mass contribution can be obtained directly from the HI surface photometry given the well known distance of the galaxy.

In Corbelli E. et. al. (2014) the DM density was derived using the detailed maps of the stellar surface-density in connection with a standard fit (via χ^2 minimization) of the total RC. The mass model considered, includes a stellar plus a gaseous disk, and a dark halo mass. The latter is assumed with a NFW or alternatively, with a URC-halo radial density profile, both with two free parameters to fit. Their results indicate that both models give a satisfactory fit, even though the fit using the NFW profile for dark matter is slightly better. The DM halo density profile cannot be uniquely determined: the main reason being that the luminous matter still significantly contributes to the total gravitational potential in the inner parts of the galaxy. Only for spirals or dwarfs with maximum velocities $< 70 \text{ km s}^{-1}$ the RC directly measures the DM profile. In objects like M33, instead, even the small uncertainties left in modelling the stellar disk mass, propagate into the inferred DM halo profile and can move the values of the best fit model from the cored to the cuspy side.

To constrain the DM density distribution in normal galaxies one can use a second scheme in which the kinematics is very weakly correlated with the (somewhat uncertain) distribution of luminous matter (Salucci P. et. al. 2010). This method, discussed in Salucci P. et. al. (2010), was applied first to the Milky Way and then to the spiral galaxy NGC 3198 (Karukes E. V. et. al. 2015). In short words, it allows to derive very precisely the DM density in the outskirts of a galaxy when the circular velocity is well known up to its first derivative, so that $\delta V/V < 0.05$, $\delta d \log V / d \log r < 0.1$ and the HI surface density is observed.

The paper is organized in four sections. In Sec.(2) we present the three main luminous matter components of the galactic disk, with their corresponding surface mass densities, and it is devoted to summarize the observed rotation curve and the baryonic disk contribution to it. We also summarize the main results of the previous dynamical analysis (Corbelli E. et. al. 2014). In Sec.(3) we develop a local modelling technique that does not rely on any of the previously global mass modeling of the galaxy to obtain a very robust and careful determination of the DM halo density of M33, and finally, Sec.(4) summarizes the main conclusions of this work.

2 LUMINOUS AND DARK MATTER CONTRIBUTIONS TO THE ROTATION CURVE

In this section we summarize the structural properties of the stellar and gaseous components of the galactic disk of M33 and we discuss its surface mass density radial-dependence as derived by Corbelli *et al.* (2014), used to fit the RC of M33.

2.1 Stellar and gaseous disks

Thanks to the tight correlations between the color and the apparent stellar mass-to-light ratio M/L (Bell *et al.* 2001), the stellar mass, to a first approximation, can be determined using multi-band optical imaging measurements of the whole galaxy luminosity. However, due to likely radial variations of the stellar mass-to-light ratio, as galaxy disks grow with time, Portinari *et al.* (2010); Zibetti *et al.* (2009); González Delgado *et al.* (2014) have been using chemo-photometric models for a large samples of spatially resolved, disk-dominated galaxies. A radially decreasing mass-to-light ratio was found based on galaxy color gradients and spectral synthesis techniques. Being M33 the second closest spiral, Corbelli *et al.* (2014), implemented an extension of the ZCR09 method to obtain a detailed map of the stellar surface mass density using mosaic maps in the B , V , I , g and i bands from the Local Group Survey (Massey *et al.* 2006) and from the Sloan Digital Sky Survey (York *et al.* 2000). After processed the images, a pixel-by-pixel synthesis model of the stellar population was performed, to obtain the stellar mass map of the M33 disk out to 5 kpc. This showed a clear radial gradient of the mass-to-light ratio in the inner regions, consistent with the negative radial metallicity gradient which supports an inside-out formation scenario. This results underlines the importance of carrying out a careful analysis of the stellar mass distribution in disks before computing their contribution to rotation curves (Portinari *et al.* 2010). By fitting the resulting radial averages of the stellar surface mass density of M33, with analytic functions, namely exponential functions with different scale-lengths r_s , Corbelli *et al.* (2014) obtain the following approximation for the radial distribution of the stellar mass surface density $\sigma_s(r)$ in units of $M_\odot \text{pc}^{-2}$:

$$\sigma_s(r) = \begin{cases} \exp(-2.010 r + 6.24), & 0.0 \text{ kpc} < r \leq 0.3 \text{ kpc}; \\ \exp(-1.239 r + 6.01), & 0.3 \text{ kpc} < r \leq 0.77 \text{ kpc}; \\ \exp(-0.758 r + 5.64), & 0.77 \text{ kpc} < r \leq 1.85 \text{ kpc}; \\ \exp(-0.515 r + 5.19), & 1.85 \text{ kpc} < r \leq 10 \text{ kpc}; \\ \exp(-0.161 r + 1.65), & 10 \text{ kpc} < r \leq 23 \text{ kpc}, \end{cases} \quad (1)$$

where r is the radial coordinate given in kpc. The fits to the radial distribution of the stellar mass density are shown in Fig.(1), where we can notice the drop of the stellar mass density by more than 3 orders of magnitudes from the center to the outskirts of the M33 disk. The amplitude of $\sigma_s(r)$ is uncertain by a 30%, while its radial trend has negligible uncertainties. As in Corbelli *et al.* (2014), in order to compute the dynamical contribution of the stellar mass density to the rotation curve, we consider the stellar disk perpendicular to the galactic plane as a flaring disk with a radially varying half thickness of only 100 pc at the center but as high as 1 kpc at the outer disk edge.

The gaseous disk is made of atomic and molecular gas (hydrogen and helium). The high resolution 21-cm data of M33 for the atomic hydrogen gas, the relative best fitting tilted ring model, and the radial averages of the HI surface density distribution, $\sigma_{HI}(r)$, have been presented by Corbelli *et al.* (2014). For the dynamical contribution of the gaseous disk to the rotation curve, the gaseous disk has been considered vertically thick with half thickness of $h = 0.5$ kpc.

As regard the baryonic matter, the chemo-photometric method provides a quite accurate determination of the stellar surface density, we can realize and then use the fact that, in the innermost parts of the galaxy ($r \lesssim 7$ kpc), see Fig.(1), it dominates over the gaseous surface density. Moreover, in the approximate range: $7 \text{ kpc} \lesssim r \lesssim 10 \text{ kpc}$, stars and the atomic gas have a similar mass surface density and beyond 10 kpc, they decrease with the radius in a similar way. It is useful to recall how in Corbelli *et al.* (2014) these derived mass distributions were used for the standard RC fitting method.

The stellar and gaseous disk contributions add in quadrature to fit the RC as follows:

$$V_d^2(r) = \Upsilon V_s^2(r) + V_g^2(r), \quad (2)$$

where $\Upsilon = \Upsilon_*/\Upsilon_*^{\text{Corbelli}} = M_*/M_*^{\text{Corbelli}}$, is the ratio between the stellar disk mass and that given by Eq.(1), which is $4.9 \times 10^9 M_\odot$ out to $r = 23$ kpc. The parameter Υ takes into account the uncertainties in the derivation of the stellar disk mass and hence, the total stellar disk mass is allowed to vary in the interval $3.4 - 6.4 \times 10^9 M_\odot$. The terms $V_s(r)$ and $V_g(r)$ indicate the contributions to the rotation curve of the stellar disk, as given by of Eq.(1), and of the Helium corrected HI and H_2 gas mass (Corbelli *et al.* 2014).

2.2 Dark matter halo models and dynamical analysis of the rotation curve

The dynamical analysis of the rotation curve is done by modelling the galaxy with a DM halo and a stellar and gaseous disks with the surface densities as discussed above in the radial range: $0.24 \leq r \leq 23$ kpc, b. Two different DM halo

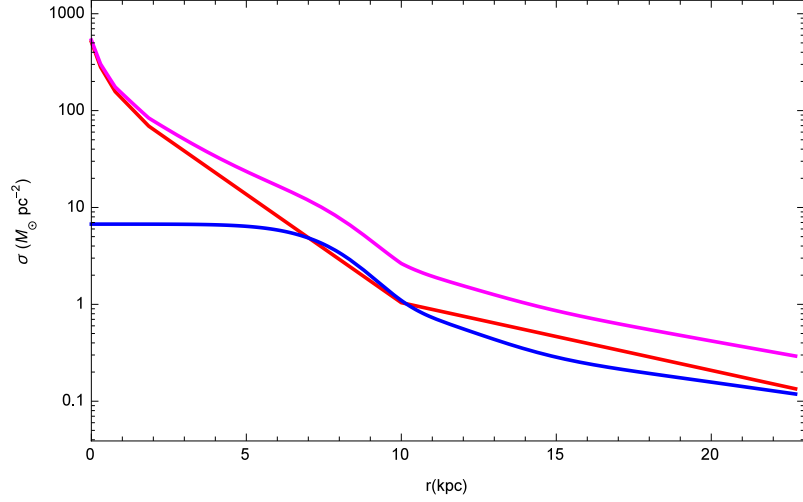


Figure 1. (color online) Radial dependence surface densities of the disk of M33: stellar (red), neutral hydrogen HI (blue) and total luminous matter: stars, atomic and molecular Hydrogen plus Helium (1.33 factor) corrected density (magenta).

models were considered by [Corbelli E. et. al. \(2014\)](#). The DM NFW density profile for structures growing in a Λ -CDM hierarchical universe ([Navarro J. F. et. al. 1996, 1997](#); [Klypin A. et. al. 2001](#); [Hayashi E. et. al. 2004](#); [Diemand J. et. al. 2005](#); [Caimmi R. et. al. 2004](#)) given by:

$$\rho_{NFW}(r) = \frac{\rho_c}{\frac{r}{r_c} \left(1 + \frac{r}{r_c}\right)^2}, \quad (3)$$

where ρ_c and r_c are the two usual halo parameters. The contribution of the DM density profile adds in quadrature to the disk contribution to give the total rotational velocity as

$$V^2(r) = V_{NFW}^2(r) + V_d^2(r), \quad (4)$$

$$V_{NFW}^2(r) = \frac{4\pi G \rho_c r_c^2}{r/r_c} \left(\ln(1 + r/r_c) - \frac{r/r_c}{1 + r/r_c} \right). \quad (5)$$

The virial mass M_{vir} and the concentration parameter $c = r_{\text{vir}}/r_c$, are related to ρ_c and r_c by:

$$\rho_c = \frac{97.2}{3} \frac{c^3}{\ln(c+1) - \frac{c}{c+1}} \rho_{\text{crit}} \text{ g cm}^{-3}, \quad (6)$$

$$r_c = \frac{1}{c} \left(\frac{3}{97.2} \frac{M_{\text{vir}}}{4\pi \rho_{\text{crit}}} \right)^{1/3} \text{ kpc}. \quad (7)$$

where r_{vir} is the virial radius and $\rho_{\text{crit}} = 9.3 \times 10^{-30} \text{ g cm}^{-3}$ is the critical density of the Universe. The free parameters, c and M_{vir} were determined as independent parameters, but after the RC fit, the authors checked the consistency of their values with the relations obtained by numerical simulations of structure formation in a Λ -CDM universe. The free parameters of this halo model: M_{vir} and c , are in fact not independent from each other ([Bullock J. S. et. al. 2001](#)). Recent simulations ([Dutton A. A. et. al. 2014](#)) suggest a correlation relation, expressed using the dimensionless value of Hubble Parameter $h = 0.678$ ([Ade P. A. R. et. al. 2016](#)) as:

$$c = 10.6 \left(\frac{1}{10^{12} h^{-1}} \frac{M_{\text{vir}}}{M_{\odot}} \right)^{-0.097}. \quad (8)$$

[Corbelli E. et. al. \(2014\)](#) obtained: $c = (9.5 \pm 1.5)$, $M_{\text{vir}} = (4.3 \pm 1.0) \times 10^{11} M_{\odot}$, and $M_{\star}^{\text{Corbelli}} = (4.8 \pm 0.6) \times 10^9 M_{\odot}$ by considering a composite probability, which takes into account the fit to the RC, the synthesis models of the stellar population and the c - M_{vir} relation found by numerical simulations.

The second halo profile we consider is the phenomenological cored density distribution, that successfully fits individual RCs (e.g. [Gentile G. et. al. \(2005\)](#) and references therein), as well as the universal rotation curve of spirals. This cored halo profile, also known as the Burkert halo profile ([Burkert A. 1995](#); [Salucci P. et. al. 2000](#)) has a radial density distribution given by

$$\rho_{URC}(r) = \frac{\rho_c}{\left(1 + \frac{r}{r_c}\right) \left(1 + \frac{r^2}{r_c^2}\right)} \quad (9)$$

where ρ_c and r_c are the central density and the core radius respectively. This density profile induces a gravitational potential such that every particles in the galactic disk rotates with a velocity V_{URC} : which adds in quadrature to the barionic disk

component:

$$V^2(r) = V_{URC}^2(r) + V_d^2(r), \quad (10)$$

$$V_{URC}^2(r) = \frac{2\pi G \rho_c r_c^2}{r/r_c} \left(\ln(1 + r/r_c) + \ln \sqrt{1 + (r/r_c)^2} - \tan^{-1}(r/r_c) \right). \quad (11)$$

The central core density ρ_c and the scaling radius r_c are not independent, as it was shown in [Donato F. et. al. \(2009\)](#):

$$\log \left(\frac{\rho_c r_c}{\text{M}_\odot \text{pc}^{-2}} \right) = 2.15 \pm 0.2. \quad (12)$$

[Corbelli E. et. al. \(2014\)](#) performed the dynamical analysis of the M33 RC with the aid of the stellar mass distribution given by the BVI maps and found the best fitting values of the parameters as: $r_c = 7.5$ kpc, $\rho_c = 18.0 \times 10^6 \text{ M}_\odot \text{ kpc}^{-3}$ and $\text{M}_*^{\text{Corbelli}} = 7.2 \times 10^9 \text{ M}_\odot$, with an acceptable global χ^2 , although larger than the best fit χ^2 , values for a NFW DM profile. Therefore, even for this galaxy, despite we have accurate extended data concerning the whole gravitational potential as well as a good determination of the mass associated to the luminous components, both DM mass models are acceptable and the best fit solution is quite degenerate. This can be easily attributed to the fact that in M33, even beyond 10 kpc, the influence of the luminous matter is not negligible so that any derivation of the DM density profile would be fraught with the uncertainties inherent to such a component. More precisely, since in the inner regions $r \lesssim 2R_D$ (being R_D the disk length scale) of most spirals, the stellar disk dominates over the dark component, even small uncertainties in the mass determination of the former induces large uncertainties in the values of the structural parameters of the dark components. By using a second method for fitting the RC data in the next section we hope to alleviate this degeneracy. We will see that the fit related to the second method is less dependent on the luminous matter distribution and thus hopefully it will help us to clarify better the properties of the DM halo that hosts M33.

3 MODEL-INDEPENDENT METHOD FOR LOCAL DENSITY ESTIMATION.

A new method to determine the DM density distribution in spiral galaxies has been introduced by [Salucci P. et. al. \(2010\)](#). This method was applied first to estimate the value of the DM density at the Sun's location ([Salucci P. et. al. 2010](#)), and extended in [Karukes E. V. et. al. \(2015\)](#) to the study of the DM distribution in the galaxy NGC 3198. The goal of this section is to derive, for the spiral galaxy M33, a model independent DM density using this method which deals with the RC at large radii, where the influences of the stellar and gaseous disks are weak.

3.1 The local density estimation method

The idea, brought by [Salucci P. et. al. \(2010\)](#) is to resort the equation of centrifugal equilibrium, which holds the spiral galaxies:

$$\frac{V^2}{r} = a_h + a_s + a_g, \quad (13)$$

where a_h , a_s , and a_g are the radial accelerations, generated by the DM halo, stellar and gaseous disks respectively.

Under the approximation of a spherical DM halo, we have

$$\rho_h(r) = \rho(r) - \Upsilon \rho_s(r) - \rho_g(r) = \frac{X_q}{4\pi G r^2} \frac{d}{dr} (rV^2 - r\Upsilon V_s^2 - rV_g^2), \quad (14)$$

$$\rho(r) = \frac{1}{4\pi G r^2} \frac{d}{dr} (rV^2), \quad (15)$$

$$\rho_s(r) = \frac{1}{4\pi G r^2} \frac{d}{dr} (rV_s^2), \quad (16)$$

$$\rho_g(r) = \frac{1}{4\pi G r^2} \frac{d}{dr} (rV_g^2), \quad (17)$$

where X_q is a factor correcting the spherical Gauss law used above in case of an oblate DM halo and it takes values between 1.05 and 1.00 (see details in [Salucci P. et. al. \(2010\)](#)), $V(r)$ is the velocity given by the RC, V_s and V_g are the stellar and gas velocities and Υ the usual stellar mass-to-light ratio. The strength of this method lies in the fact that we have transformed the surface mass density of the stellar and gaseous disks in equivalent bulk densities with the aid of Gauss's law. Since the velocities induced by the stellar and gaseous disks decrease slowly after 9.53 kpc, we expect a sharp fall for their equivalent three-dimensional densities ρ_s and ρ_g , and we are just left only with the DM contribution to the observed RC. From this fact, we can infer the DM halo properties directly from the experimental data.

An issue left to treat is to derive an analytical expression for the total velocity $V(r)$ from the available discreet set of the observational points of the experimental RC. Having an analytic function will avoid artifact due to the numerical computation

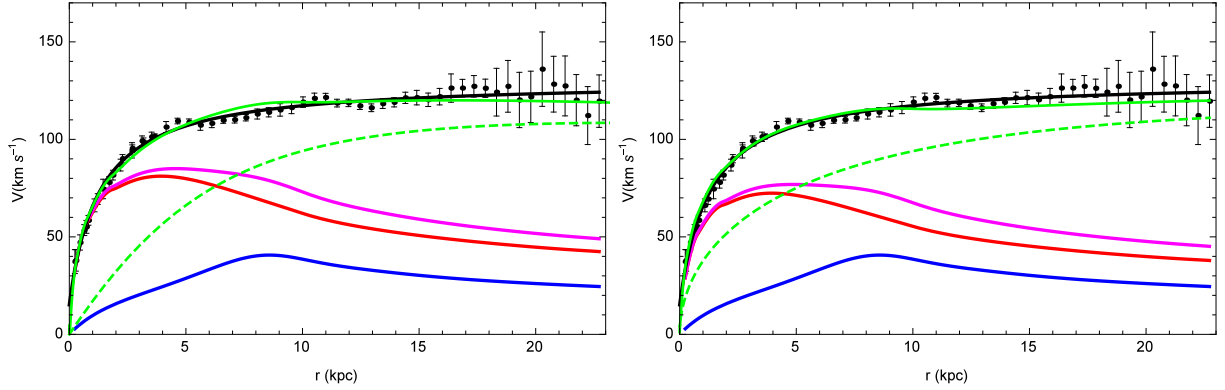


Figure 2. (color online) RC of M33 (black dots with error bars) with the best fitting model given by the empirical velocity profile Eq.(18) (continuous black line). In both panels (with green lines) are also shown, for comparison, the URC (left panel) and the NFW (right panel) solutions, as discussed in the previous section. The stellar (red), gas (blue) and total disk (magenta) contributions are shown as well.

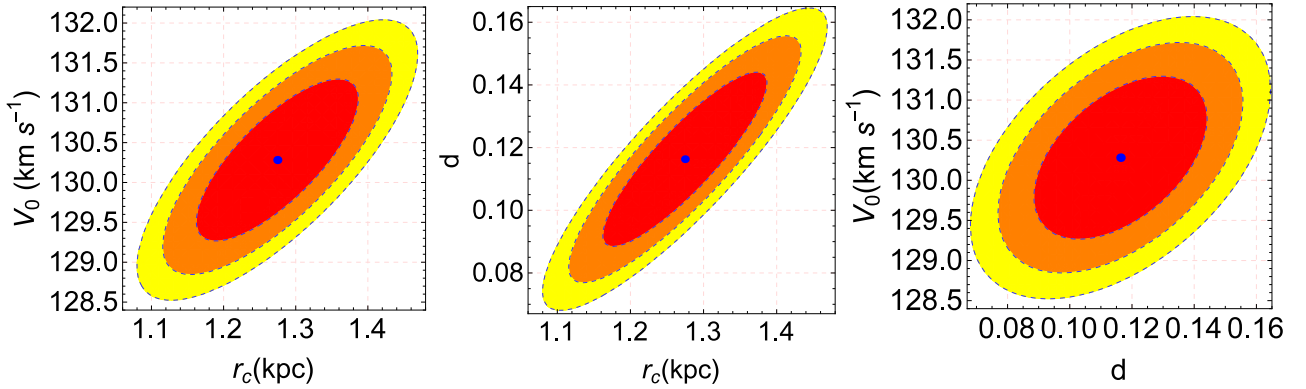


Figure 3. (color online): 1, 2 and 3 σ confidence ellipses (red, orange and yellow) for the best fitting parameters V_0 , r_c , d . The blue central points indicate the best fitting values.

of the derivative of $V(r)$ needed for the computation of the total density as given by Eq.(15). The next subsection is devoted to find an appropriate empirical smooth curve to solve this problem.

3.2 Empirical velocity profile

With the aid of the local density method, we can study, directly from the experimental data, the DM halo properties by computing the densities given by Eq.(15), Eq.(16) and Eq.(17) respectively. Just with the purpose of deriving a smooth profile of dV/dr , we introduce the following an empirical velocity formula to describe the rotation curve of M33 :

$$V(r) = V_0 \frac{r/r_c + d}{r/r_c + 1}. \quad (18)$$

This is a simple, rational, 3-parameter-dependent velocity profile that reproduces at large galactocentric distances a flat velocity curve and as we will see immediately, it describes genuinely the RC in the range allowed by the experimental data. The three free parameters, namely V_0 the terminal velocity, r_c the scaling radius and $d < 1$, an additional parameter to prevent $V(r)$ to be constant, make the degree of freedom of the fit to be similar to that of the first method (see previous Section) when considering the uncertainties on the stellar surface mass density. In addition, the empirical velocity formula can be used both for the URC halo plus luminous disk and the NFW halo plus luminous disk mass models.

By minimizing the χ^2 distribution for fitting the RC data with its measurement errors, with the above analytic function, we obtain the best fit parameters: $V_0 = (130.2 \pm 1.0) \text{ km s}^{-1}$, $r_c = (1.3 \pm 0.1) \text{ kpc}$, and $d = (0.12 \pm 0.03)$, giving a $\chi^2_{\text{red}} = 0.75$. In Fig.(2) we show the fit to the RC data of the derived analytic function. For comparison we show also the fits obtained by Corbelli *et al.* (2014) using the URC DM profile (left panel) and the NFW DM profile (right panel) discussed in the previous section. In Figs.(3) we show the 1, 2, 3 σ confidence levels for such three free parameters.

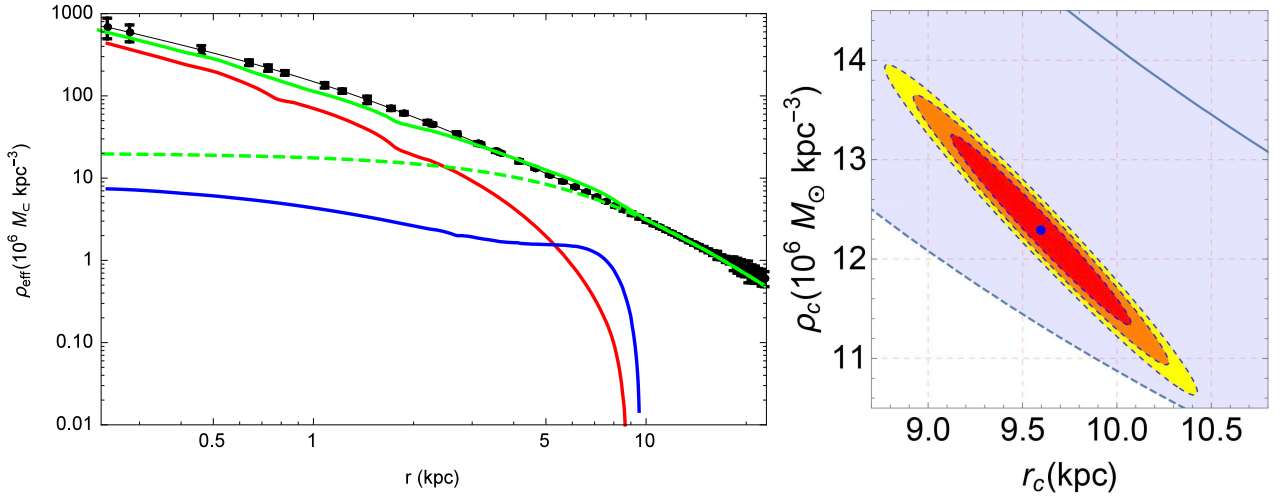


Figure 4. (color online) The left panel shows the dependence on the galactic radius of the different effective densities: the continuous black line with points and error bars corresponds to $\rho(r)$ as derived from Eq.(15); in red and blue colors are plotted the effective densities of stars and gas given by Eq.(16) and Eq.(17) respectively. The green dashed line represents the best fitting URC DM halo, while the continuous green line represents the total contribution of the obtained URC halo plus stars and gas. The right panel shows the 1, 2 and 3 σ confidence ellipses (red, orange and yellow) for the best fitting parameters r_c and ρ_c respectively, as well as the correlation relation between these two (blue continuous line) given by Eq.(12) with a 20% of uncertainty (shaded blue area).

3.3 Dark matter profiles and effective densities

Given the goodness of the fit of RC data with the analytic function given by Eq.(18) the goal of this subsection is to use this continuous smooth curve to compute $\rho(r)$ as given by Eq.(15) and the effective baryonic disk densities. As mentioned before, for $r \gtrsim 9$ kpc in Eq.(14), the contributions of the star and gas densities are negligible and we are left only with the DM halo contribution.

In the range of galactocentric distances $9.5 \text{ kpc} \leq r \leq 22.72 \text{ kpc}$, we fit the derived density profile using the URC and NFW DM radial density distribution. In the case of the URC profile, we obtain the best fitting values: $r_c = (9.6 \pm 0.5) \text{ kpc}$ and $\rho_c = (12.3 \pm 1.0) \times 10^6 \text{ M}_\odot \text{ kpc}^{-3}$ respectively, giving a $\chi^2_{\text{red}} = 0.8$ and the halo virial mass is $M_{\text{vir}} = (3.0 \pm 0.8) \times 10^{11} \text{ M}_\odot$. In Fig.(4) (left panel) is shown the corresponding fit in log-log scale. Framed by this solution, let us stress again that nearly around $r \sim 9.2 - 9.55 \text{ kpc}$ the stars and gas contributions drop sharply more than two orders of magnitude, therefore, in the radial range $9.53 \text{ kpc} \leq r \leq 22.72 \text{ kpc}$ the stellar mass-to-light ratio Υ plays no role in this analysis and we can obtain the two halo parameters also if the total disk mass has some uncertainties. In the right panel of Fig.(4) we show the corresponding 1, 2, 3 σ confidence levels for the two halo parameters. The blue continuous line in the same panel shows the correlation found by numerical simulations for these parameters (Eq.(12)) and the blue shaded area its 1 σ region. Clearly the solution obtained for the parameters ρ_c and r_c lie inside the error margins given by the correlation, as reported in Donato F. et. al. (2009).

We performed the same analysis using the NFW profile. In this case we obtained the best fitting values $c = (9.5 \pm 0.7)$ and $M_{\text{vir}} = (5.4 \pm 0.6) \times 10^{11} \text{ M}_\odot$, giving a $\chi^2_{\text{red}} = 1.0$. In the left panel of Fig.(6) we show the corresponding fit in log-log scale. In the right panel we display the corresponding 1, 2, 3 σ confidence levels for such two free parameters of the NFW profile, as well as the correlation relations and its uncertainties as given by Eq.(8) (blue shaded area).

It is worth to discuss the present result. We can trace the distribution of matter in M33 using the RC observational data starting from $r = 0.24 \text{ kpc}$. Below this radius, no information can be inferred except by extrapolating the best fitting models, which later can be tested using higher resolution observations. In the radial range $0.24 \text{ kpc} \leq r \lesssim 9 \text{ kpc}$, the stellar component is very relevant with respect to the DM halo component. For both DM halo models tested, the structural parameters of the DM distribution are mingled with the unknown value of the disk mass. In both cases, no information can be extracted either since any measurements of DM distribution would be fraught with the uncertainties due to the stellar contribution (i.e. the stellar disk accounts for most of the total gravitational potential of the galaxy). Around 9 kpc, the luminous matter still competes against DM to dominate over the total mass given the uncertainties of the circular velocity. But beyond 9.5 kpc, at $\simeq 3.5R_D$, the exponential decrease of the stellar matter density and the negligible contribution of the gaseous component, which never plays a role even if its total mass is about half of that of the stars, assure that only the DM component balances the radial accelerations, which the gaseous disk is engaged with.

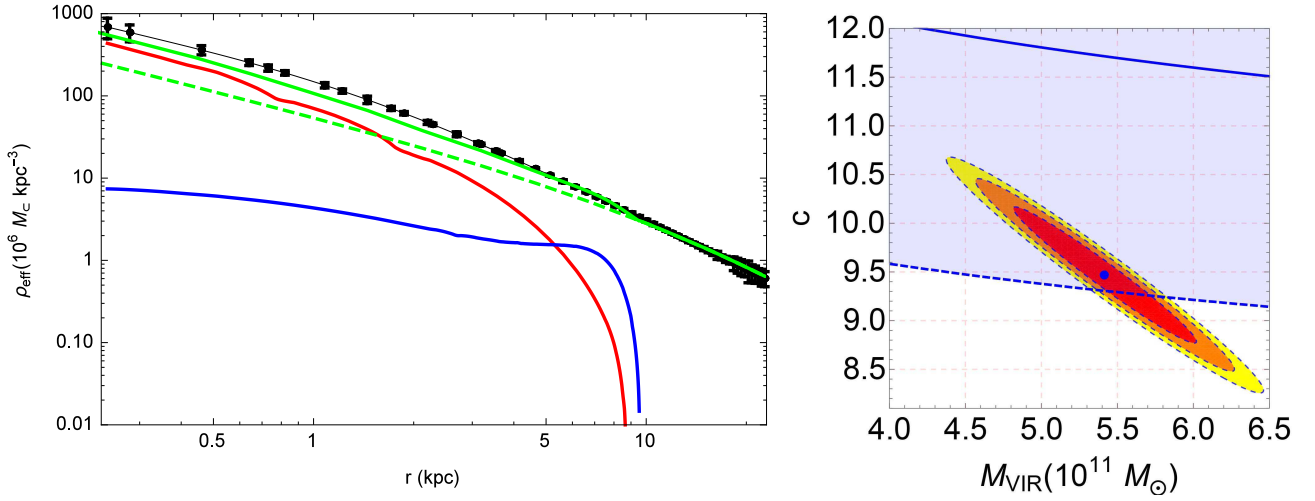


Figure 5. (color online) The left panel shows the dependence on the galactic radius of the different effective densities: the continuous black line with points and error bars corresponds to $\rho(r)$ as derived from Eq.(15) which describes our data; in red and blue colors are plotted the stars and gas effective densities given by Eq.(16) and Eq.(17) respectively. The green dashed line shows the best fitting curve considering the NFW DM halo, while the continuous green line represents the total contribution of the obtained NFW halo profile plus stars and gas. The right panel shows the 1, 2 and 3σ confidence ellipses for the best fitting halo parameters c and M_{vir} respectively, where the blue central point corresponds to the best fitting values of c and M_{vir} . The continuous blue line (shaded blue area) in the right panel corresponds to the $c - M_{\text{vir}}$ correlation Eq.(8) $c = 13.8^{+3.6}_{-2.8} (M_{\text{vir}}/10^{11} M_{\odot})^{-0.097}$.

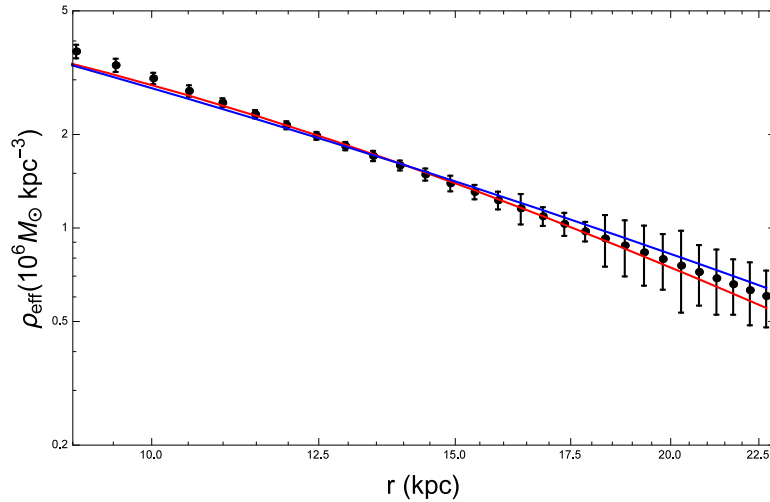


Figure 6. (color online) Comparison between the observed DM halo density profile (black dots with error bars) and the obtained URC (red) and NFW (blue) solutions in the range of $9.53 \text{ kpc} \leq r \leq 22.72 \text{ kpc}$.

4 CONCLUSIONS

In this paper we deepened the results of Corbelli *E. et. al.* (2014) which obtained a global fit of the RC of M33, after an accurate mass modelling of its stellar disk and by considering a DM halo with a cuspy NFW or a cored URC profile. The results of the global fit to the RC favour a cuspy Λ -CDM halos despite a cored one is still compatible with the data. In this paper we have followed a new approach to study the DM content of M33. Relying on the centrifugal equilibrium condition, assuming a spherical halo, we trace the properties of the DM halo only by the experimental RC. This method, used also by Salucci *P. et. al.* (2010) and Karukes *E. V. et. al.* (2015), relies on fitting the dark matter density distribution of M33 in the radial range $9.53 \text{ kpc} \leq r \leq 22.72 \text{ kpc}$, where the stellar and gaseous contributions to the RC are negligible. According to this method, the URC profile with the following parameters: $r_c = (9.6 \pm 0.5) \text{ kpc}$ and $\rho_c = (12.3 \pm 1.0) \times 10^6 M_{\odot} \text{ kpc}^{-3}$ which corresponds to a halo mass of $M_h = (6.7 \pm 1.2) \times 10^{10} M_{\odot}$ provides an excellent fit to the M33 rotation curve. Therefore, with the analysis presented in this paper, the possibility that M33 harbors a cored dark matter halo seems still suitable. Even though the determination of the stellar disk mass via synthesis models has eliminated most of the disk-halo degeneracies in

this low luminosity spiral, we have shown that the cuspy or cored dark matter density profiles degeneracy still hold because of the possible different methodologies in modelling RC data.

References

- Ade P. A. R. *et al.* [Planck Collaboration], *Astron. Astrophys.* **594** (2016) A13 [arXiv:1502.01589 [astro-ph.CO]].
- Athanassoula E., Bosma A. and Papaioannou S., *Astron. Astrophys.* **179**, 23-40 (1987), [arXiv:9903432].
- Avila-Reese V., Colin P., Valenzuela O., D’Onghia E. and Firmani C., *Astrophys. J.* **559** (2001) 516, [arXiv:0010525].
- Bell E. F. and de Jong R. S., *Astrophys. J.* **550** (2001) 212, [arXiv:0011493].
- Bosma, A., PhD Thesis, Groningen Univ., 1978, [arXiv:0009161].
- Bosma A. and van der Kruit P. C., *Astron. Astrophys.*, **79** (1979) 281-286, [arXiv:0009161].
- Bullock J. S., Kolatt T. S., Sigad Y., Somerville R. S., Kravtsov A. V., Klypin A. A., Primack J. R. and Dekel A., *Mon. Not. Roy. Astron. Soc.* **321** (2001) 559, [arXiv:9908159].
- Burkert A., *IAU Symp.* **171** (1996) 175, *Astrophys. J.* **447** (1995) L25, [arXiv:9504041].
- Caimmi R. and Marmo C., *Serb. Astron. J.* **169** (2004) 11, [arXiv:0406585].
- Chan T. K., Kereš D., Oñorbe J., Hopkins P. F., Muratov A. L., Faucher-Giguère C.-A. and Quataert E., *Mon. Not. Roy. Astron. Soc.* **454** (2015) no.3, 2981 [arXiv:1507.02282 [astro-ph.GA]].
- Cole S. and Lacey C. G., *Mon. Not. Roy. Astron. Soc.* **281** (1996) 716, [arXiv:9510147].
- Corbelli E., *Mon. Not. Roy. Astron. Soc.* **342** (2003) 199 [astro-ph/0302318].
- Corbelli E. and Waltherbos R. A. M., *Astrophys. J.* **669** (2007) 315, [arXiv:0707.2162].
- Corbelli E., Thilker D., Zibetti S., Giovanardi C. and Salucci P., *Astron. Astrophys.* **572** (2014) A23, [arXiv:1409.2665].
- de Blok W. J. G. and Bosma A., *Astron. Astrophys.* **385** (2002) 816, [arXiv:0201276].
- Diemand J., Zemp M., Moore B., Stadel J. and Carollo M., *Mon. Not. Roy. Astron. Soc.* **364** (2005) 665, [arXiv:0504215].
- Donato F. *et al.*, *Mon. Not. Roy. Astron. Soc.* **397** (2009) 1169, [arXiv:0904.4054].
- Dutton A. A. and Macciò A. V., *Mon. Not. Roy. Astron. Soc.* **441** (2014) no.4, 3359, [arXiv:1402.7073].
- Eke V. R., Navarro J. F. and Steinmetz M., *Astrophys. J.* **554** (2001) 114, [arXiv:0012337].
- Gentile G., Salucci P., Klein U., Vergani D. and Kalberla P., *Mon. Not. Roy. Astron. Soc.* **351** (2004) 903, [arXiv:0403154].
- Gentile G., Burkert A., Salucci P., Klein U. and Walter F., *Astrophys. J. Lett.* **634** (2005) L145, [arXiv:0506538].
- González Delgado R. M. *et al.* [CALIFA Collaboration], *Astron. Astrophys.* **562** (2014) A47, [arXiv:1310.5517].
- Hayashi E. *et al.*, [arXiv:0408132].
- Karukes E. V., Salucci P. and Gentile G., *Astron. Astrophys.* **578** (2015) A13, [arXiv:1503.04049].
- Klypin A., Kravtsov A. V., Bullock J. and Primack J., *Astrophys. J.* **554** (2001) 903, [arXiv:0006343].
- Macciò A. V., Dutton A. A. and Bosch F. C. v. d., *Mon. Not. Roy. Astron. Soc.* **391** (2008) 1940, [arXiv:0805.1926].
- Marinoni C., Monaco P., Giuricin G. and Costantini B., *Astrophys. J.* **521** (1999) 50, [arXiv:9903394].
- Massey P., Olsen K. A. G., Hodge P. W., Strong S. B., Jacoby G. H., Schlingman W. and Smith R. C., *Astron. J.* **131** (2006) 2478, [arXiv:0602128].
- Navarro J. F., Frenk C. S. and White S. D. M., *Astrophys. J.* **462** (1996) 563, [arXiv:9508025].
- Navarro J. F., Frenk C. S. and White S. D. M., *Astrophys. J.* **490** (1997) 493, [arXiv:9611107].
- Palunas P. and Williams T. B., *Astron. J.* **120** (2000) no.6, 2284, [arXiv:0009161].
- Persic M. and Salucci P., *Mon. Not. Roy. Astron. Soc.* **234** (1988) 131.
- Portinari L. and Salucci P., *Astron. Astrophys.* **521** (2010) A82, [arXiv:0904.4098].
- Rubin V. C., Thonnard N. and Ford W. K., Jr., *Astrophys. J.* **238** (1980) 471.
- Salucci P. and Persic M., *Astron. Astrophys.* **351** (1999) 442, [arXiv:9903432].
- Salucci P. and Burkert A., *Astrophys. J.* **537** (2000) L9, [arXiv:0004397].
- Salucci P., Nesti F., Gentile G. and Martins C. F., *Astron. Astrophys.* **523** (2010) A83, [arXiv:1003.3101].
- Syer D. and White S. D. M., [arXiv:9611065].
- York D. G. *et al.* [SDSS Collaboration], *Astron. J.* **120** (2000) 1579, [arXiv:0006396].
- Zibetti S., Charlot S. and Rix H. W., *Mon. Not. Roy. Astron. Soc.* **400** (2009) 1181, [arXiv:0904.4252].

This paper has been typeset from a \LaTeX file prepared by the author.